33rd Annual International Conference of the IEEE EMBS
Boston, Massachusetts USA, August 30 - September 3, 2011

System Identification of Mechanomyograms Detected with an Acceleration Sensor and a Laser Displacement Meter

Takanori Uchiyama and Keita Shinohara

***Abstract*— The purpose of this study is to investigate the transfer functions of mechanomyograms (MMGs) detected with an acceleration sensor and a laser displacement meter. The MMGs evoked by electrical stimulation to the peroneal nerve were recorded on the skin of the tibial anterior muscle. The displacement MMG (DMMG) and the acceleration MMG (AMMG) systems were identified using a singular value decomposition method. The appropriate order of the AMMG system was six and that of the DMMG system was four. The undamped natural frequencies of the systems were compared to resonance frequencies of human soft tissue. Some of the undamped natural frequencies estimated from the AMMG systems agreed with the resonance frequencies in the literature but others were lower than the resonance frequencies. The undamped natural frequencies estimated from the DMMG systems were lower than the resonance frequencies.**

I. Introduction

A mechanomyogram (MMG) provides unique information about muscle contraction. For example, an integrated MMG increases and then decreases as the contraction level increases [1]. This property reflects the recruitment of motor units and the fusion of the contractile force of the motor units. If the transfer function of the MMG system were identified, the coefficients of the transfer function could provide another important property, the visco-elasticity of the muscle.

The MMG has been measured with various transducers such as an acceleration sensor [2], [3], piezoelectric crystal contact sensor [4], [5], condenser microphone [6], [7], and laser displacement meter [8], [9], each of which detects different quantities. The condenser microphone and laser displacement meter detect the displacement of the skin, while the acceleration sensor detects the acceleration of the skin. We suppose that this difference affects the identified transfer function. In this study, we applied the singular value decomposition method to the MMGs detected with an acceleration sensor (AMMG) and a laser displacement meter (DMMG) in order to identify the MMG systems.

II. Methods

A. Measurement of MMGs

MMGs of the tibial anterior muscle were evoked by stimulating the common peroneal nerve electrically and were measured with an acceleration sensor and a laser displacement meter (Fig. 1). Six healthy male subjects aged 22 to 25 participated in the experiment. All subjects provided informed consent. Each subject sat on a chair, and his foot, ankle, knee, and thigh were fixed on the experimental equipment. The common peroneal nerve was stimulated with 31 mono-polar-rectangle pulses 500 μs in width and inter-pulse intervals of 0.6 s. The strength of the stimulation was adjusted in order to obtain 100, 75, 50, 25, and 10% of the peak-to-peak values at a supramaximal stimulus. First, a DMMG was measured with a laser displacement meter (LK-G80, Keyence, Osaka, Japan). The measurement point, $L/3$, from the caput fibulae was adjusted in order to observe the maximum amplitude of the DMMG where L is the distance between the caput fibulae and the lateral malleolus. The sensitivity of the laser displacement meter was 0.5 V/mm. The DMMG was sampled at 2000 Hz and stored on a personal computer.

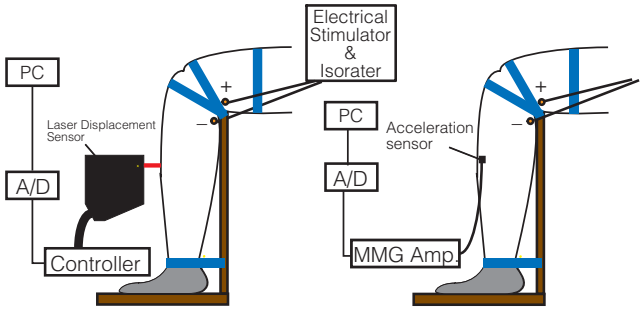

Fig. 1. Schematic illustration of the experimental setup

Next, an AMMG was measured with an acceleration sensor (MP110-10-110, Medisens, Sayama, Saitama, Japan). The acceleration sensor was attached on the measurement point of the skin with adhesive tape. The acceleration was amplified (1 V/G) and filtered (1–250 Hz), and the AMMG was sampled at 2000 Hz and stored on a personal computer.

B. System Identification

Twenty-six evoked MMGs, from the sixth to thirty-first, were synchronously averaged. The lag time from the electrical stimulation to the onset of the MMG was determined when the amplitude was three times greater than the standard deviation of the background. The MMGs excluding the lag time were used for system identification. The DMMG was decimated because of its low frequency range, and its sampling rate was 200 Hz. There were 1200 samples for the AMMG, and 120 samples for the DMMG.

The singular value decomposition method was applied to identify the system, the input of which is an ideal impulse

T. Uchiyama is with Faculty of Science and Technology, Keio University, Yokohama, Japan uchiyama@appi.keio.ac.jp
K. Shinohara is with Graduate School of Science and Technology, Keio University, Yokohama, Japan shino-k@bi.appi.keio.ac.jp

and the output of which is the DMMG or AMMG. The system is described as a state equation,

$$\begin{cases} \boldsymbol{x}(k+1) &= \boldsymbol{A}\boldsymbol{x}(k) + \boldsymbol{B}u(k) \\ y(k) &= \boldsymbol{C}\boldsymbol{x}(k) + Du(k), \end{cases} \tag{1}$$

where $u(k)$ is an input, $y(k)$ is an output, and $\boldsymbol{x}(k)$ and $\boldsymbol{x}(k+1)$ are state variables. The transfer function $G(z)$ was calculated as

$$G(z) = \boldsymbol{C}^T(z\boldsymbol{I} - \boldsymbol{A})^{-1}\boldsymbol{B} + D. \tag{2}$$

The performance of the identified system was evaluated by the fitness P,

$$P = 100 \times \left\{ 1 - \sqrt{\frac{\sum_{k=1}^{N}(\hat{y}(k) - y(k))^2}{\sum_{k=1}^{N}(y(k) - \bar{y})^2}} \right\}, \tag{3}$$

where $y(k)$ is the observed MMG, $\hat{y}(k)$ is the estimated MMG, and $\bar{y}$ is the average of the observed MMG. The model order was determined by P and the gain characteristics of the transfer function at the main frequency band of the MMG.

C. Undamped Natural Frequency

The transfer function was factorized to the products of the first- and the second-order models depending on the poles of the transfer function. The discrete second-order models were converted to the continued one using the zero-order hold. The continued second-order model was compared to the standard form of the second-order model,

$$\frac{\omega_n}{s^2 + 2\zeta\omega_n s + \omega_n^2}, \tag{4}$$

where ω_n is the undamped natural frequency and ζ is the damping ratio. The undamped natural frequency was calculated and compared to the resonance frequency of human soft tissue according to the literature, although the undamped natural frequency is not strictly identical to the resonance frequency and the undamped natural frequency is slightly higher than the resonance frequency.

III. Results and Discussion

A. AMMG

Fig. 2 shows typical examples of the AMMG (Subject A). The model order was six. The left panel, a, shows the observed and estimated AMMGs at a contraction level of 10%. The red and blue lines denote the observed and estimated AMMGs, respectively. The peak amplitude and time were well estimated by the singular value decomposition method, while the second negative and the fifth positive peaks of the estimated AMMG were smaller than those of the observed AMMG. The right panel, b, shows the observed and estimated AMMGs at a contraction level of 100%. The AMMG was also well estimated. The fitness was larger than that at a contraction level of 10%.

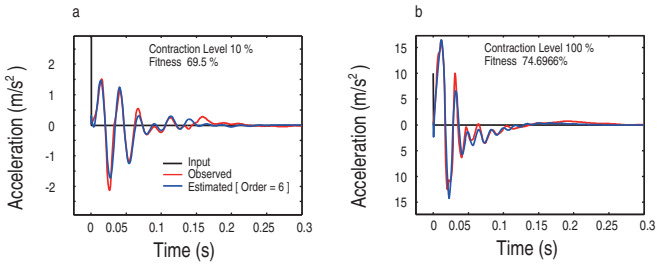

Fig. 2. Typical examples of the AMMG (Subject A, sixth-order model). (a) contraction level 10%, (b) contraction level 100%

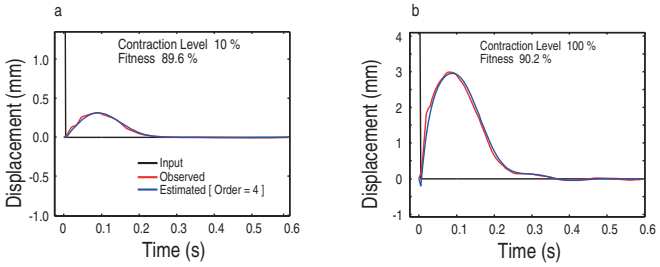

Fig. 3. Typical examples of the DMMG (Subject A, fourth-order model). (a) contraction level 10%, (b) contraction level 100%

B. DMMG

Fig. 3 shows typical examples of DMMGs (Subject A, fourth-order model). The left panel, a, shows the observed and estimated DMMGs at a contraction level of 10%. The red and blue lines denote the observed and estimated DMMGs, respectively. A single broad peak was observed while five or more peaks were observed in the AMMG. The DMMG was well estimated and the fitness was 89.6%, which is higher than that of the AMMG at the same contraction level. The right panel, b, shows the MMGs at a contraction level of 100%. The MMGs were also well estimated.

C. Undamped Natural Frequency

The AMMG and DMMG were well estimated with the sixth- and forth-order models, respectively. Therefore, the AMMG was factorized to three second-order models, and the DMMG was factorized to two second-order models. Table I shows the undamped natural frequencies calculated from the AMMG at various contraction levels. The frequencies were arranged in descending order.

The highest frequencies, f_1, increased as the contraction level increased. The values were within the range of the resonance frequencies estimated from the mechanical impedance of human soft tissue [10]. Some of the middle frequencies, f_2, were within the range of the resonance frequencies, but others were lower than the resonance frequencies. The frequencies did not show as clear a tendency as that shown by the increase of the contraction level. The lowest frequencies, f_3, were lower than the resonance frequencies.

Table II shows the undamped natural frequencies calculated from the DMMG at various contraction levels. The frequencies were also arranged in descending order. Both

TABLE I

UNDAMPED NATURAL FREQUENCY ESTIMATED FROM AMMG (HZ)

(%)	f_1	f_2	f_3
10	40.7 ± 0.3	28.5 ± 0.4	0.1 ± 0.0
25	43.6 ± 1.8	31.2 ± 1.2	5.0 ± 0.2
50	43.4 ± 0.5	16.9 ± 0.8	0.4 ± 0.0
75	53.4 ± 3.1	13.3 ± 14.5	0.7 ± 0.0
100	60.8 ± 4.2	40.6 ± 4.9	3.8 ± 2.8

TABLE II

UNDAMPED NATURAL FREQUENCY ESTIMATED FROM DMMG (HZ)

(%)	f_1	f_2
10	4.7 ± 1.0	2.4 ± 0.4
25	5.1 ± 0.4	2.7 ± 0.4
50	5.3 ± 0.4	3.1 ± 0.1
75	5.7 ± 0.1	2.8 ± 0.0
100	5.7 ± 0.1	2.8 ± 0.0

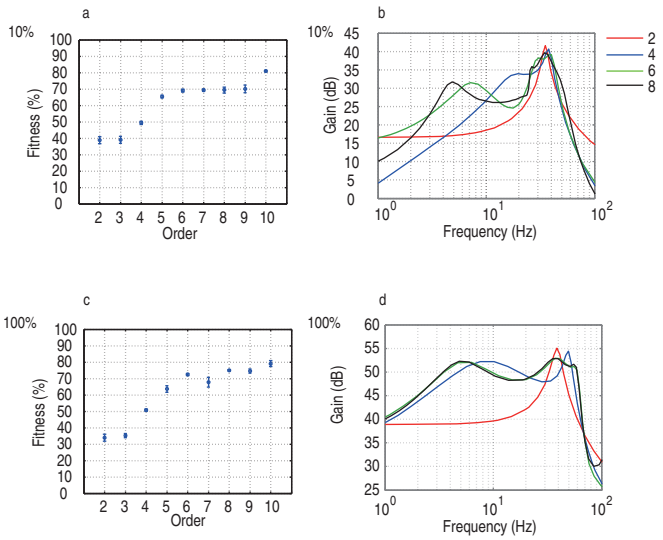

Fig. 4. Fitness and gain characteristics of various order models of the AMMG (Subject A). (a) fitness of the model at a contraction level of 10%, (b) gain characteristics of the model at a contraction level of 10%, (c) fitness of the model at a contraction level of 100%, (d) gain characteristics of the model at a contraction level of 100%

of the undamped natural frequencies, f_1 and f_2, were lower than the resonance frequencies and were close to the lowest frequencies, f_3, of the AMMG.

We suppose that the differences in the model order and the undamped natural frequency are caused by the differences in the quantities detected with the transducers. The acceleration sensor detects an acceleration, which is the second differential of the displacement. The second differential operator in Laplace transforms is s^2; therefore, compared to that of the displacement, the gain characteristics of the acceleration are enhanced where the enhancement is proportional to the square of the frequency. Compared with the laser displacement meter, the acceleration sensor is more sensitive to the high-frequency component, which facilitates the identification of the high undamped natural frequency component of the AMMG system.

D. Model Order

Fig. 4 shows the fitness and gain characteristics of various order models of the AMMG. The top left panel, a, shows the relationship when the contraction level was 10%. The fitness was almost constant at the order of six to nine. The top right panel, b, shows the gain characteristics of the various order models. The green line denotes the gain characteristics of the sixth-order model. The characteristics were close to the gain characteristics of the eighth-order model denoted by the black line. The bottom left panel, c, shows the relationship at the contraction level of 100%. The fitness was also constant at the order of six to nine. The bottom right panel, d, shows the gain characteristics. The characteristics of the sixth-order model, denoted by the green line, coincided with those of the eighth-order model, denoted by the black line. If the models provided the same performance, the low-order model would be suitable to describe the system. As a result, we chose the sixth-order model for the AMMG.

Fig. 5 shows the fitness and the gain characteristics of the DMMG. The top panels, a and b, show the fitness and the gain of various order models at the contraction level of 10%. The fitness was almost constant at the fourth- or higher-order models. The gain characteristics of the fourth-order model denoted by the blue line agreed with those of the sixth-order model denoted by the green line at 10 Hz or less, which is the dominant frequency of the DMMG. The bottom panels, c and d, show the gain characteristics at the contraction level of 100%. The fitness was also constant at the fourth- or higher-order models, and the gain characteristics of the fourth-order model agreed with those of the sixth-order model. Therefore, we chose the fourth-order model for the DMMG.

The undamped natural frequencies of the DMMG were close to each other. The fitness of the second-order model of the DMMG, while high (80% or more), was slightly lower than that of the fourth-order model. Moreover, the sixth-order model of the AMMG provided one low undamped natural frequency close to those of the DMMG. Although further study is necessary, the second-order model might be appropriate for the DMMG.

The order of the DMMG system was lower than that of the AMMG system. The undamped natural frequency of the DMMG system was lower than the resonance frequency of human soft tissue, which implies that the DMMG provides only macroscopic lateral expansion of the muscle while the AMMG provides inner microscopic vibration at a high frequency superimposed on the macroscopic expansion.

IV. CONCLUSIONS

The system of MMGs detected with an acceleration sensor and a laser displacement meter was identified using a singular value decomposition method. The appropriate orders of the AMMG and the DMMG were six and four, respectively. The undamped natural frequencies of the AMMG were close to the resonance frequencies reported in the literature, while those of the DMMG were lower than the resonance frequencies.

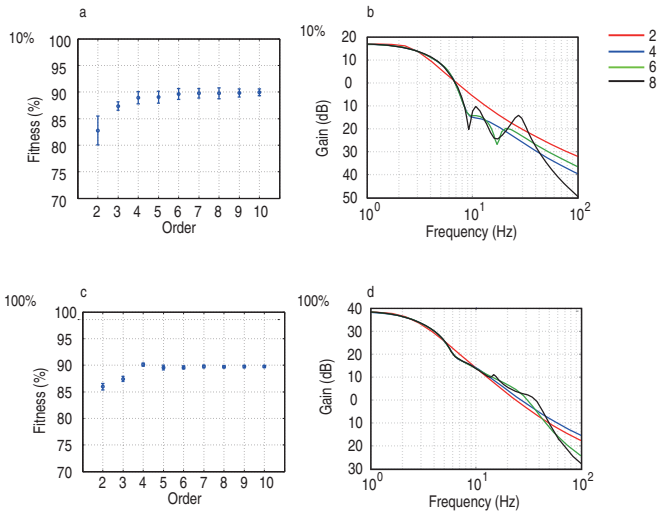

Fig. 5. Fitness and gain characteristics of various order models of the DMMG (Subject A). (a) fitness of the model at a contraction level of 10%, (b) gain characteristics of the model at a contraction level of 10%, (c) fitness of the model at a contraction level of 100%, (d) gain characteristics of the model at a contraction level of 100%

ACKNOWLEDGMENTS

This work was supported by Grant-in-Aid for Scientific Research.

REFERENCES

[1] K. Akataki, K. Mita, M. Watakabe, K. Itoh, Mechanomyogram and force relationship during voluntary isometric ramp contractions on the biceps brachii muscle, *Eur. J. Appl. Physiol.*, vol. 84, 2001, pp. 19–25.

[2] C. Orizio, D. Liberati, C. Locatelli, D. De Grandis, A. Veicsteinas, Surface mechanomyogram reflects muscle fibres twitches summation, *J. Biomech.*, vol. 29, 1996, pp. 475–481.

[3] C. Cescon, M. Gazzoni, M. Gobbo, C. Orizio, D. Farina, Non-invasive assessment of single motor mechanomyographic response and twitch force by spike-triggered averaging, *Med. Biol. Eng. Comput.*, vol. 42, 2004, pp. 496–501.

[4] J. T. Cramer, T. J. Housh, J. P. Weir, G. O. Johnson, J. M. Bernig, S. R. Perry, Gender, muscle, and velocity comparisons of mechanomyographic and electromyographic responses during isokinetic muscle actions, *Scand. J. Sci. Sports*, vol. 14, 2004, pp. 116–127.

[5] T. K. Evetovich, T. J. Housh, J. R. Stout, Mechanomyographic responses to concentric isokinetic muscle contraction, *Eur. J. Appl. Physiol.*, vol. 75, 1997, pp. 166–169.

[6] M. Shinohara, M. Kouzaki, T. Yoshihisa, T. Fukunaga, Mechanomyography of the human quadriceps muscle during incremental cycle ergometry, *Eur. J. Appl. Phyisol.*, vol. 76, 1997, pp. 314–319.

[7] M. Watakabe, K. Mita, K. Akataki, Y. Itoh. Mechanical behaviour of condenser microphone in mechanomyography, *Med. Biol. Eng. Comput.*, vol. 39, 2001, pp. 195–201.

[8] P. Kaczmarek, J. Celichowski, H. Drymala-Celichowska, A. Kasiński, The image of motor units architecture in the mechanomyographic signal during the single motor unit contraction: *in vivo* and simulation study, *J. Electromyogr. Kinesiol.*, vol.19, 2009, pp. 553-563.

[9] C. Orizio, R. V. Baratta, B. H. Zhou, M. Solomonow, Force and surface mechanomyogram relationship in cat gastrocnemius, *J. Electromyogr. Kinesiol.*, vol. 9, 1999, pp. 131–140.

[10] H. Oka, T. Yamamoto, Dependence of biomechanical impedance upon living body structure, *Med. Biol. Eng. Comput.*, vol. 25, 1987, pp. 631–637.